Spatiotemporal dynamics of optical molecular motors

Edeltraud Gehrig* and Ortwin Hess†
Advanced Technology Institute, School of Electronics and Physical Sciences, University of Surrey, Guildford, Surrey GU2 7XH, United Kingdom
(Received 15 April 2003; published 22 August 2003)

The spatiotemporal dynamics of optical molecular motors is simulated on the basis of a spatially resolved model. A spatially dependent Fokker-Planck model for the molecular motors is linked with Maxwell's wave equation describing the external excitation via a spatially inhomogeneous light field. Simulations show that strong diffusion of the embedding fluent leads to increased motor dynamics while in inhomogeneous ensembles motor clustering may occur. Spatially inhomogeneous optical excitation may provide a means of movement control of the molecular motors.

DOI: 10.1103/PhysRevE.68.021914 PACS number(s): 87.16.Nn, 87.10.+e, 05.40.−a

I. INTRODUCTION

Recent investigations in the biosciences that involve, e.g., single-molecule nanomanipulation of biomolecules [1], have revealed a large variety of fascinating effects. One of these phenomena is the existence of ''microscopic engines''—highly specialized functional units (macromolecules) that can consume energy to induce motion and to generate forces. Depending on their specific dynamics and function these molecular motors or motor proteins may be classified as linear and rotary motors [2–4]. Supplying energy to linear molecular motors produces movement along a filamentous structure. Examples for linear molecular motors are the movement of myosin along an actin filament [5,6], kinesin [7] and dynein [8] along a microtubule, and RNA polymerase along DNA [9]. Typically the filaments are formed by a polymerization process from identical (asymmetric) monomers leading to a polar regular and periodic structure. The motor molecule can attach to a protein filament which then serves as a track for its motion. The interaction of the motors with the filament can be described by potentials that reflect the periodic structure along the filament surface. In the presence of an energy source (e.g., adenosine triphosphate, ATP) the motor may then move in a direction defined by the polarity of the track. The complex dynamics of molecular motors therefore covers many length and time scales. A motor that is bound to a filament can—after consumption of a fuel molecule—move in steps of the order of several nanometers. Making about a hundred such steps in its bound state the motor typically covers a walking distance that is of the order of micrometers. On larger length scales the motor undergoes random walks which consist of alternating sequences of bound and unbound motor states, i.e., of directed walks along the filaments and nondirected diffusion in the sourrounding medium (e.g., an aequeous solution).

Various physical models [10–26] have been suggested to describe this fascinating generation of force and motion by molecular motors. These models may be grouped in continuous [12,27,28] and discrete [29,30] models. Continuous model descriptions are based on a numerical integration of a set of Fokker-Planck equations [12,31]. There, the nonequilibrium rectifying processes that can induce macroscopic motion of a particle can be introduced as fluctuating forces, fluctuating potentials, and particle fluctuations between states [12]. The transition rates for particles between the respective energies are thereby integrated using a detailed balance approach [32]. Discrete theories, on the other hand, describe the motors as rigid particles. They are often analytically solvable but the introduction of an external force is difficult to handle [32]. The compatibility of discrete and continuous models has been investigated in Refs. [32,33]. Single-particle Brownian motor models [11,34] and coupled-particle models [35–38] were used to study noise-induced motion as well as the interaction of elastically coupled particles. The influence of collective effects has been considered and analyzed in various descriptions [12,20,37,39–41]. Furthermore, the interplay of the biochemical cycle and the conformational state could be included in theoretical studies [30]. The different conformations have been simulated by introducing internal states for the motors [30,42]. We note that one thereby typically introduces an average density of particles on the expense of disregarding the explicit influence of and dependence on the spatial extension of the system.

Next to the mechanicochemical coupling within a motor ensemble it is, in particular, the interaction with an external energy source (e.g., electromagnetic waves) that plays an important role in the function of molecular motors. In fact, many experimental techniques (fluorescence microscopy, optical tweezers, etc.) directly exploit the fact that light exerts force on matter. It is thus of fundamental interest to analyze the fundamental interactions between light and molecules. So far, only few theoretical studies have been established that describe the interaction of light with living matter: Scattering functions [43] have been derived to simulate the interaction between spatially inhomogeneous biological media and light. The spectral method [44] uses a Fourier expansion of the field amplitude. This method has successfully been applied to describe the optical properties of tissues and individual cells. The scattering of light by blood cells as well as the resulting near and far fields have been simulated utilizing the *T*-matrix theory [45]. In the discrete-dipole approximation [46], a particle is divided into subvolumes that are as-

*Electronic address: E.Gehrig@surrey.ac.uk
†Electronic address: O.Hess@surrey.ac.uk

sumed to behave as dipoles. As an alternative to the wave description of light, the Boltzmann transport equation or the time-dependent standard diffusion equation [47–49] has been used. The propagation and scattering of light in tissue could be analyzed at the cellular level by approximating the cells with monosized homogeneous spheres [50]. In contrast, the finite-difference time-domain approach [51] has the advantage of allowing the consideration of inhomogeneous objects of arbitrary shape and index distribution. This method which is based on a direct integration of Maxwell's equations has been applied to cellular-scattering problems [52,53]. The total size of the model system, however, is limited by computational considerations since the grid spacing must be a fraction of the wavelength to guarantee convergence [54].

Next to the investigation and interpretation of biomolecules, there is a growing number of artifically designed molecular motors [55–57] suggesting that the physics of these systems is relevant for microtechnical and nanotechnical devices. First theoretical approaches [58–61] to synthetic systems motors (e.g., molecular propellers, brakes, switches, shuttles) include an external chemical, electrochemical, or photochemical stimulus that induces a switching process or movement within the molecule or triggers a change in shape or assembly of molecules.

The work we present here was inspired by recent experimental demonstrations of a molecular motor system that could be controlled by optical illumination [62]. It could be shown that light-induced conformational changes allowed via an optomechanical cycle the construction of chiral optical (chiroptical) molecular switches [63] and the first light-driven molecular motor [62]. A second energy source—in addition to the difference of the chemical potentials of fuel and products in the ATP hydrolysis—may thus be represented by an applied light field that changes the internal states and/or transition rates, leading to a ''light-driven'' motor system. The spatiotemporal dynamics of this motor system will then be determined by the spatially varying light-matter coupling, dynamic excitation and relaxation of the particles, as well as a characteristic (nonlinear) response of the particles to the light field. Depending on a particular excitation configuration one might even think of a spatial optical grating [64] designed by e.g., crossedbeams for the selective excitation or guiding of a molecular ensemble.

Up to now, many spatiotemporal effects that are involved in real molecular motor systems still are not fully understood: How strongly does the local state of a molecular motor (characterized, e.g., by its individual diffusion process or internal energetic state) influence the dynamics of its molecular neighbors? And to what extent do spatial fluctuations in molecular properties as well as spatial diffusion and transport—resulting in characteristic spatial distributions and molecular densities of detached and attached motors—affect the function and properties of a motor system?

To lay the basis for an analysis of this spatiotemporal dynamics occurring on a mesoscopic scale, we propose to extend the existing model descriptions with respect to a direct consideration of the spatial and temporal degrees of freedom. We consider the spatiotemporal dynamics of an ensemble of molecular motors interacting with filaments in a spatially inhomogeneous biological medium. Aiming at describing linear biological motor proteins that move along a linear filament, we consider a model system of processive motor molecules characterized by a sawtooth potential for the ground and the excited state, respectively. The dynamics of these motors is then determined by the currents resulting from the space-dependent potentials, by a spatially varying excitation of motors from the lower to the upper state (which we assume to occur via spatially inhomogeneous external illumination) as well as by spatiotemporal fluctuations. By direct numerical integration of the partial differential equations of motion the model allows a very natural and straightforward representation of spatial inhomogenieties in the ensemble of molecular motors as well as the spatiotemporally varying nonequilibrium dynamics and interaction of bound (i.e., attached to, e.g., a filament) and free (i.e., diffusive motion in surrounding fluent) molecular motors.

II. THEORETICAL DESCRIPTION

In the light of the optically excited molecular motor recently demonstrated in Ref. [62] we here construct a model system consisting of parallel filaments and linear motors subject to illumination with a coherent light field. In essence, the model combines equations of motion for the particles with a spatially dependent set of parameters describing the biological medium, its interaction with the environment and, in particular, spatiotemporal fluctuations. A characteristic parameter set thus includes the density and distribution of the particles in the medium, molecular properties (e.g., potential shapes, diffusion constants), spatially dependent optical properties (e.g., sensitivity to illumination, transition rates), and the interactions between the particles (e.g., between attached motors and their neighbors on the filament or between particles of different type) or between molecular motors and their environment (e.g., a fluent) with characteristic interaction times. The resulting equations that model the spatiotemporal dynamics of the optical molecular motors thus describe spatially varying particle densities and the dynamic coupling of those to the light-field, particle-to-particle scattering, spatially varying particle properties, as well as the interaction with the embedding material. The spatially dependent light field dynamics is simulated on the basis of Maxwell's wave equation and includes diffraction, the spatiotemporal coupling to the medium, as well as spatiotemporal light-field fluctuations.

With all generality in the theory, we will later focus on a specific model system that consists of molecular motors moving along parallel filaments (width $w=25$ nm, filament separation $s=100$ nm) in an embedding medium [see Fig. 1(a)]. Motors may either be attached to the filaments or move freely in the surrounding fluent. Our spatial resolution thereby allows, in principle, an inclusion of spatially varying geometrical parameters with fluctuations ∂w and ∂s. In the example we assume the filaments to be fixed but the inclusion of a diffusive motion of the filaments is straightforward. In order to keep the description simple and to focus on generic properties, we do not include microscopic structural

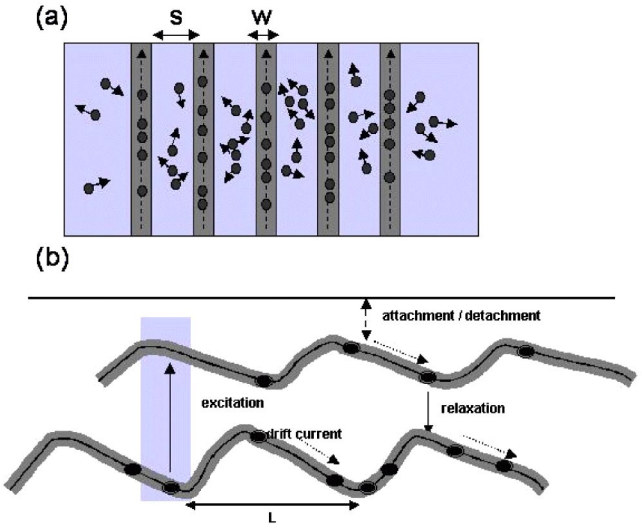

FIG. 1. (a) Scheme of the molecular model system: The spatially distributed motors are attached to the filament (here, parallel to each other) or move freely in the surrounding medium (e.g., fluent). The arrows indicate the diffusive motion in the environment (line) and the interaction between attached and free motors as well as between motors from neighboring filaments via dynamic detachment and attachment. (b) The states of the motors (here, two) are simulated with (shifted) potential shapes V_i with a characteristic periodicity L and a fluctuation ∂V. According to the potential the drift currents drive the motors into the respective potential minimum. From there the motor molecules may be excited in a particular spatiospectral regime into the excited level where they continue their downhill movement to the next potential minimum of the corresponding high-energy state.

details of the biological motor proteins but consider the biochemical cycle and the conformational state to be interdependent [11,28]. This separation of time scales [12] is justified by the fact that the various microscopic degrees characterizing the motor proteins relax on time scales shorter than the typical relevant time scales for the chemical cycle.

In our theory the motor system is represented by particle densities which can be in one of N internal states (representing, e.g., the steps of the chemical cycle) [10–12,14,28], for example, a ground state and an excited state (see Fig. 1). We use a spatially dependent Fokker-Planck description and introduce distribution functions for the probability to find a motor of a particle ensemble at time t in state i at position $\mathbf{r}$ in the two-dimensional space representing the filament ensemble. For each state i, the particle is subject to a polar periodic pontential $V_i(\mathbf{r},t)$ of average period L. The motors dynamically detach from and attach to the filaments. The transition rates $\kappa_{ji}(\mathbf{r})$ are spatially dependent; they are influenced by, e.g., ATP concentration [65] or external illumination. The detachment will be represented with spatially and temporally dependent detachment rates that may depend on the spatially varying potential shape as well as on a spatially dependent external force. The distribution of attached motors (in state i) is then given by the following evolution equations:

$$\frac{\partial}{\partial t}p_i(\mathbf{r},t) = -\nabla j_i(\mathbf{r},t) + \Gamma_{\infty i}(\mathbf{r})p_\infty(\mathbf{r},t) + \sum_{j\neq i}\kappa_{ji}(\mathbf{r})p_j(\mathbf{r},t)$$

$$-\Gamma_{i\infty}(\mathbf{r})p_i(\mathbf{r},t) - \sum_{j\neq i}\kappa_{ij}(\mathbf{r},t)p_i(\mathbf{r},t), \qquad (1)$$

with current j_i, transition rates for ''in scattering'' $[\kappa_{ji}(\mathbf{r})]$ and ''out scattering'' $[\kappa_{ij}(\mathbf{r})]$ and attachment as well as detachment rates $\Gamma_{\infty i}(\mathbf{r})$ and $\Gamma_{i\infty}$, respectively. Thereby, the rates may have any time and space dependence. We thus do not have to restrict ourselves to, e.g., a δ-shaped detachment rate near the maxima of the potential: the full spatial and temporal dependence can be taken into account via the spatial and temporal integrations. The currents j_i representing the source terms in Eq. (1) result from diffusion, interaction with the filament, and the action of a possible external force F. They are defined by

$$j_i(\mathbf{r},t) = -\mu_i(\mathbf{r})\{k_bT\nabla p_i(\mathbf{r},t) + [\nabla V_i(\mathbf{r},t) - F(\mathbf{r},t)]p_i(\mathbf{r},t)\}$$

$$V_i(\mathbf{r},t) = \sum_m v_i^m \sin(\omega_m t + \phi_m) + \delta V_i(\mathbf{r},t). \qquad (2)$$

In Eq. (2) μ_i is the particle mobility. In most model descriptions the potential shapes $V_i(\mathbf{r},t)$ are considered as ''ideal,'' i.e., with constant periodicity and identical energetic shift between the potential energy of the sublevels characterizing the motor ensemble. Furthermore, the transition and detachment rates usually are localized in a region of particular size and minimum values elsewhere. We note that we keep our spatiotemporally resolved description as general as possible here and explicitly include a spatial dependence of the potential shape and the transition rates. In our simulations, however, we later will approximate the potentials using a sum of sin functions with spatially dependent amplitudes. The spatial variation is included via a space-dependent fluctuation term $\delta V_i(\mathbf{r},t)$ that we simulate with a Gaussian distribution. We further would like to note that in principle any arbitrary potential shape (not necessarily a sawtooth shape) and any perturbation (arbitrary function of space and time, e.g., specific local excitations) can be included and analyzed with respect to its influence on the motor dynamics. For simplicity, however, we will consider in the following a two-level system, i.e., assume that the motors may be either in a lower, ''ground,'' or ''excited'' level.

A motor, which initally lies in a potential minimum of the lower state, gets excited into the higher state, where it diffuses. It then undergoes nondirected diffusive motion in the surrounding aqueous solution until it encounters the same or another filament to which it can rebind and continue its directed walk. The diffusion of free motors is described by

$$\frac{\partial}{\partial t}p_\infty(\mathbf{r},t) = -\nabla j_\infty + \sum_i \Gamma_{i\infty}(\mathbf{r})p_i(\mathbf{r},t) - \sum_i \Gamma_{\infty i}(\mathbf{r})p_i(\mathbf{r},t),$$

$$j_\infty = -\mu_\infty(\mathbf{r})[k_bT\nabla p_\infty(\mathbf{r},t) - F(\mathbf{r},t)p_\infty(\mathbf{r},t)]. \qquad (3)$$

Next to the force induced by the conformational changes, additional forces induced by light illumination may act on

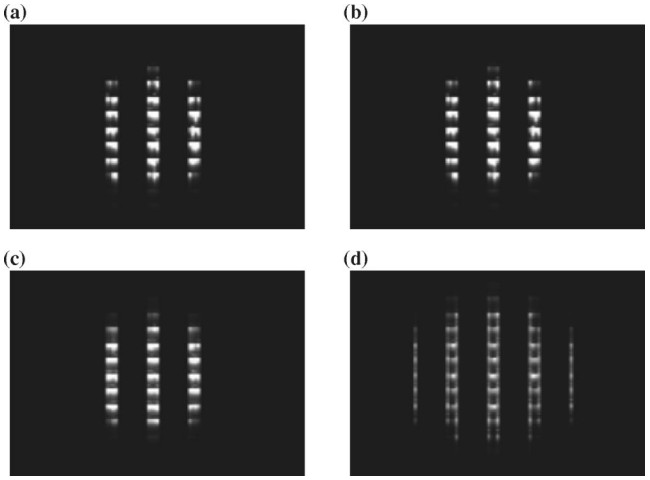

FIG. 2. Snapshots [(a,c), 5 ms, (b,d), 40 ms)] of the spatial motor distribution with a diffusion constant in the fluent of (a,b) $D_f^{free}=5D_f^{attached}$ and (c,d) $D_f^{free}=50D_f^{attached}$.

our model system. They can be included via two ways: First, a light field may shift the potential of a particular molecular state. This would lead to changes in the spatially dependent potential. Second, light may alter the transition rates between the various sublevels of the system. In principle, these transition rates can be derived from standard chemical kinetics given by, e.g., the ADP/ATP reaction. More generally the transition rates may by perturbed by any means, for example, in the case of artificially constructed systems by photon fluxes, which may induce state changes provided an appropriate frequency range were chosen. Depending on energetic bandwidth and intensity the excitation may induce a transfer of motors that have accumulated in the potential minima characterizing a molecular state into an excited state of higher energy. In combination with the resulting molecular ''relaxation'' of motors from the potential minimum of the higher state into the low-energy state, this may then—depending on the characteristic time scales for detachment and attachment—increase the forward movement of the motors (see Fig. 2).

External excitation via a light field can be considered with wave equations describing the spatially dependent illumination and light propagation. The dynamics of the light fields can be calculated within the frame of Maxwell's wave equation:

$$\frac{n_l}{c}\frac{\partial}{\partial t}\mathbf{E}(\mathbf{r},t)=iD_p\nabla_T^2\mathbf{E}(\mathbf{r},t)-\frac{1}{2}\int_\omega d\omega\,\alpha(\mathbf{r},t)\mathcal{E}(\omega)+E_{inject}(\mathbf{r},t),$$

$$\alpha(\mathbf{r},t)=-\sum_{i,j}\left[\kappa_{ij}(\mathbf{r},t)p_j(\mathbf{r},t)-\kappa_{ji}(\mathbf{r},t)p_i(\mathbf{r},t)\right],$$

$$\kappa_{ij}(\mathbf{r},t)=\kappa^0(\mathbf{r},t)\frac{\gamma^2}{(\omega_{ij}-\omega_0)^2+\gamma^2}\mathcal{E}(\omega_{ij}),$$

$$\mathbf{E}(\mathbf{r},t)=\int_\omega d\omega\mathcal{E}(\omega). \tag{4}$$

The wave equation for the description of the light-field dynamics explicitly takes into account the propagation and diffraction (D_p) of the coherent light signal in the medium as well as the dynamic interaction via a spatiospectral coupling to the medium [including the modification of the signal induced by the medium, $\alpha(\mathbf{r},t)$]. We thereby assume a frequency-dependent light-induced variation of the intralevel transition rates $\kappa_{ij}(\mathbf{r},t)$ which we approximate with a Lorentzian line shape function. In our model system we chose the dependence of these rates on the molecular potential such that they complement the movement of the motors induced by the drift currents. According to their potential dependence the drift currents lead to an accumulation of motors in the potential minima. We consequently chose the transition rate from the ground to the excited level to be maximum in the potential mimima of the potential of the low-energy (ground) state of the motor. The transition rate from the excited level to the ground level is set to the minimum of the potential of the excited state. $\kappa^0(\mathbf{r},t)$ represents the unperturbed transition rates as given by the chemomechanical cycle of the system [65]. All parameters and properties may be space- and time-dependent allowing for a self-consistent inclusion of spatiotemporal fluctuations.

The spatiotemporal dynamics of the motor molecules is characterized by various regimes: First, the motors move along the filament with a typical walking distance of a few microns [66–68]. On larger time scales, the motors then undergo random walks which consist of alternating sequences of bound and unbound motor states, i.e., of directed walks along the filaments and nondirected diffusion in the environment (e.g., an aqueous solution). The character of the directed and diffusive motion, the progressivity and efficiency of the operation of molecular motors thereby depend on many parameters. There are, in particular, geometrical parameters (distribution of filament and motors), motor properties (potential shapes, diffusion times, tranistion rates), excitation conditions, and spatiotemporal fluctuations.

The explicit consideration of the various spatial and temporal degrees of freedom allows the simulation of spatiotemporal diffusion, the dynamic coupling between motors and environment and between motors of neighboring filaments, as well as the coupling between the motor ensemble and an external excitation process. In particular, the space- and time-dependent equations allow the self-consistent inclusion of spatially varying molecular properties and inhomogenious motor distributions. In the following we discuss numerical results that illustrate the model.

III. SPATIOTEMPORAL DYNAMICS

As an example we simulate the dynamics of the motor-filament system shown in Fig. 1(a). The molecular motors move along filaments (with potential period 8 nm) which in our model system are assumed to be arranged in parallel to each other in the embedding medium. Motors may either be attached to the filaments or move freely in the surrounding

fluent. The bound motors may be either in the ground or the excited state. Thereby we assume the sawtooth potential of the excited level to be shifted by half a period length with respect to the ground state. We will discuss the following three scenarios: (a) ''diffusive motors'': influence of diffusion on motor dynamics, (b) ''fluctuating motors'': motor ensembles with spatially varying motor molecules, (c) ''excited motors'': influence of a space-dependent optical excitation on motor dynamics. Thereby, typical transition rates are taken from the literature [28,32,42,65,69].

A. Diffusive molecular motors: The influence of diffusion on the motor dynamics

The diffusion of motor molecules in a filament system is determined by both, the diffusion coefficient of the motors that are attached to a filament and the diffusion coefficient characterizing the environment. In addition to this direct dependence on parameters, an indirect influence is given by the density of molecular motors and the geometry of the system under consideration (e.g., width and lateral distance of the filaments). For a normal aqueous solution, the unbound diffusion coefficient is much larger than the bound state diffusion coefficients. For example, the diffusion coefficient for kinesin in the bound state is of the order of $10^{-3}, \ldots, 5 \times 10^{-2}$ $\mu m^2 s^{-1}$ [42]. The diffusion coefficient in the surrounding medium is given by the classical Stokes-Einstein relation [42] and depends on the thermal energy, on the dynamic viscosity of the solution, and on the effective hydrodynamic radius of the motor particle. Typical values are 2.4–24 $\mu m^2 s^{-1}$. The transition rates between upper and lower levels of the motors are chosen sufficiently high to induce a transition between the two motor states. The motors that have—due to the drift current—accumulated near the potential minima of, e.g., the ground state can thus be transfered to the excited state where they continue their propagation. The parameter Γ of the transition rates is chosen such that the optical excitation occurring in direction of the potential variation has a spatial extension of $\approx 0.25 \times L$ (where L is the potential period). The attachment and detachment rates were constant.

Figure 2 shows snapshots of a model motor system with a diffusion constant of 1×10^{-3} $nm^2 s^{-1}$ of bound (i.e., moving along the filaments) motors. The diffusion constant of the free (i.e., moving in the embedding fluent) motors was set to 5×10^{-3} $\mu m^2 s^{-1}$ [Figs. 2(a,b)] and 50×10^{-3} $\mu m^2 s^{-1}$ [Figs. 2(c,d)], respectively. The snapshots were taken after 5 ms (a,c) and 40 ms (b,d). They show the sum of attached motors in ground and excited levels. In the start of the calculation the motors were assumed to be homogeneously distributed in a circular area in the center of the filament system, with equal density of bound and free motors. Immediately after the start of the calculation the periodic potential leads—via the drift currents [Eq. (2)]—to an accumulation of the motors in the respective potential minima [Figs. 2(a) and 2(c)]. With increasing time the dynamic detachment and reattachment of the motors in combination with motor diffusion leads to a characteristic irregular molecular distribution [Fig. 2(d)].

The snapshots show that the value of the diffusion in the fluent strongly affects the spatiotemporal dynamics of the system. If the diffusion constant of the free motors is small, the motor molecules move only over small distances (compared to the period length of the potential) in the embedding medium until they reattach to the filaments. As a consequence, the motors may then after reattachment find themselves in the same potential period. If, on the other hand, the embedding fluent is characterized by a higher diffusive constant, the free motors can pass a longer distance (compared to the period length of the potential) until they are bound to a filament. As a consequence, a significant fraction of the ''free'' motors then falls into the next potential period where they are again transported by the currents towards the corresponding potential minimum. As can be seen in Fig. 2(d), an increased diffusive motion in the environment may not only increase the motor velocity in the ''preferred'' (e.g., from bottom to top) propagation direction but also induce—via the coupling between bound and free motors—a backward motion and thus lead to a spatial broadening of the motor distribution. However, applying an external force F to the system the backward motion may be suppressed and the effectivity of the overall ratched effect induced by the asymmetric periodic potential may be increased. In addition to the longitudinal dynamics (i.e., along the filaments), the increased diffusion of free motors leads—via the dynamic attachment and detachment to a coupling of neighboring filaments and consequently to a spatiotemporal transfer of motor molecules into regions left and right from the initial motor distribution.

B. Fluctuating motors: Spatially inhomogeneous motor ensembles

Next, we consider a motor ensemble with spatially varying molecular properties. In the model such spatial inhomogeneities are taken into account via space-dependent parameters of the height and periodicity of the potential (δV_i). We assume a Gaussian distribution (here, with a variance of 8%). We would like to note that, in principle, every parameter can be varied and analyzed with respect to its influence on the spatiotemporal dynamics individually.

The influence of the parameter fluctuations on the dynamics of the system becomes directly apparent in the snapshots of the motor distribution. In the calculation the densities of free and bound motors were again initialized with an ideal uniform distribution. Figures 3(a)–3(c) show results of a numerical simulation for a motor ensemble with 8% fluctuation in the potential parameters. The time between successive plots is 10 ms. As can been seen from Fig. 3, a spatial variation of the molecular properties may significantly change the behavior of the system: In the motor ensemble with spatially inhomogeneous potential parameters locations near high potential steps lead to a spatial accumulation of motors. Low potential steps, on the other hand, increase the ''one-way'' propagation of the motors. The spatially inhomogeneous potential parameters lead to a space-dependent height and length of the potential step and—via Eq. (2)—to a corresponding variation in the drift currents. With increasing time,

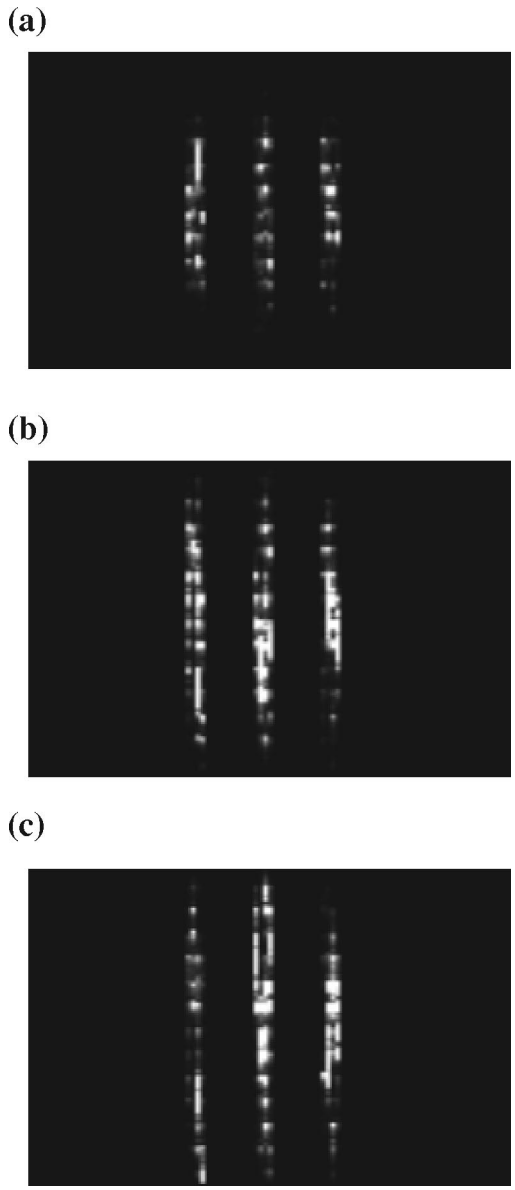

FIG. 3. Snapshot of the spatial motor distribution with spatially varying molecular properties (fluctuation amplitude of 8%). The time between successive plots is 10 ms.

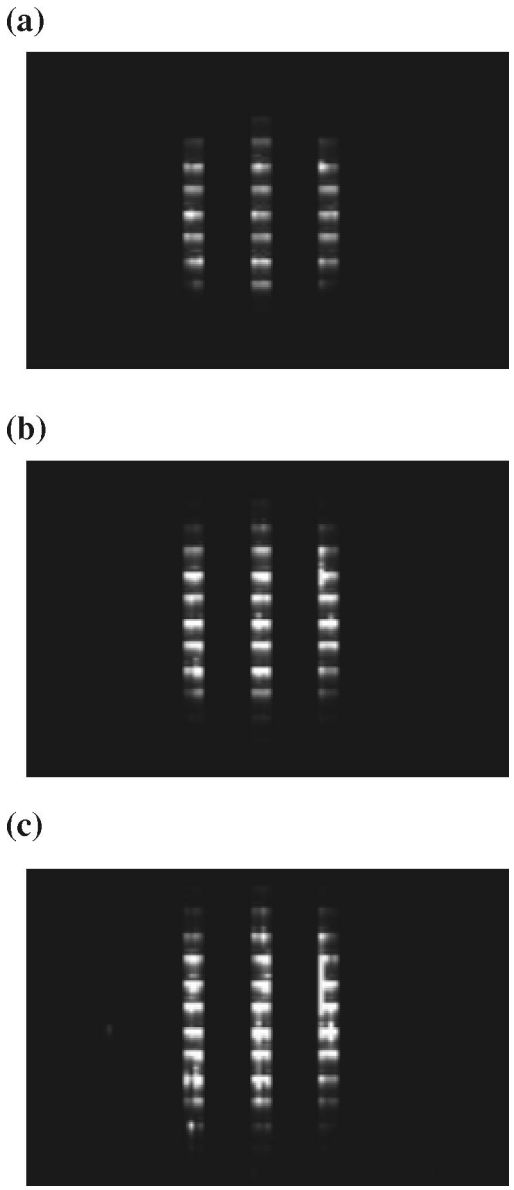

FIG. 4. Spatially dependent excitation of a motor ensemble by an adjusted coherent light field.

regions near high potential steps lead to a spatial accumulation of motors. Low potential steps, on the other hand, increase the propagation of the motors. As a consequence, the spatially varying height and periodicity of the potential lead to strongly irregular distributions and to the formation of spatiotemporal ''molecular clusters'' that can be seen in Fig. 3.

C. Excited molecular motors: The influence of optical excitation

In the following we assume that the illumination with a coherent optical light field changes the intralevel transition rates between the lower and the upper level of the motors. Depending on the frequency and energy of the light this effect may occur within a particular energetic interval [simulated with the line shape function in Eq. (A1)]. In our model the coherent light injection leads (in the area of maximum coupling at center of the beam) to an increase of a factor of 2 of the rate κ_{12} that induces a spatially and temporally varying asymmetry in the rates. The value of the width of the line function thereby determines the sharpness of the transition. In a first situation we consider the situation of localized excitation: In this example, the optical excitation induces a switch between the ground and excited states; motors in a region (with a spatial extension of $\approx 0.25L$) close to the potential minima of the ground state are transferred to the excited level and vice versa.

Figure 4 shows (in a time window of 60 ms) snapshots of the spatial distribution of molecular motors within the optically excited ensemble. The distribution was initially localized in the center of the medium. The dynamic interaction between the particle ensemble and the light fields propagat-

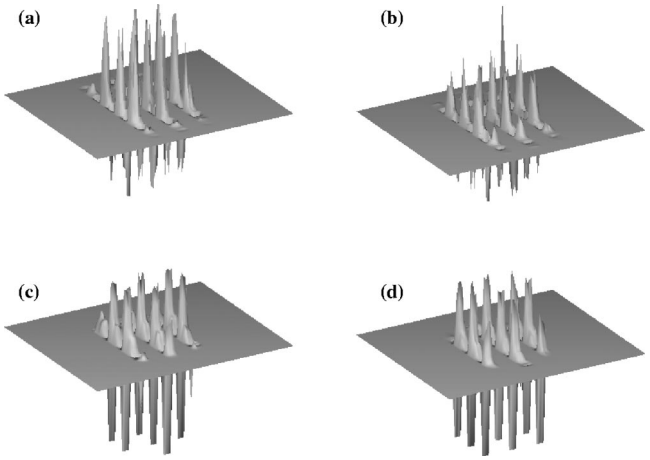

FIG. 5. Transition rates (a,b) and drift currents (c,d) for the ground-state motors in the ground level (a,c) and in the excited level (b,d).

ing in the system leads to complex spatiotemporally varying light-matter interactions. The spatially dependent optical excitation (in the example: Gaussian shaped light beam, injected from the top in the center of the molecular probe) increases the probability for a transition from the potential minimum of the ground state to the excited state level. After propagating to the next potential minimum of the excited state the motors are again transferred to the low-energy state. According to the shape of the potentials [see Fig. 1(b)], the ''relaxed'' motors may then find themselves in the potential period next to the one they started from. The selective excitation consequently transfers motors that have due to the drift current accumulated in the potential minimum of the ground state—via the excited state—to the next potential period. As can be seen in Fig. 4, this finally results in an increased motor movement. Although the calculations have been performed for an artificial system (assuming, e.g., the light-induced increase of a factor of 2 of the transition rates) they may be applied to any ''real molecular system.'' The transition rates not only change the distribution of the molecular motors but—due to their dependence on the motor densities—also the spatiotemporal distribution of the drift currents. For a visualization of this indirect mutual influence, Fig. 5 displays for the situation of Fig. 4 temporal snapshots of the transition rate difference $\Delta\kappa_i=\kappa_{ij}(\mathbf{r},t)p_j(\mathbf{r},t)-\kappa_{ji}(\mathbf{r},t)p_i(\mathbf{r},t)$ (a,b) and drift currents (c,d) of motors in the ground level, i.e., $i=1,j=2$, (a,c) and excited level, i.e., $i=2,j=1$ (b,d). All distributions are characterized by sequences of minima and maxima whose separation corresponds to the periodicity of the potential. The distributions of the excited levels show maxima where the distributions of the ground levels are minimum and vice versa—corresponding to the definitions of the potentials and to the definitions of drift currents and transition rates. Due to the spatiotemporally varying motor distributions $\Delta\kappa_1$ is not equal to $-\Delta\kappa_2$. The shape and sign of current distributions depend on shape and periodicity of the potentials. In particular, the rising parts of the potential lead to negative currents whereas the decrease of the potential determines the regions of positive drift currents [see also Fig. 1(b)]. Furthermore, a

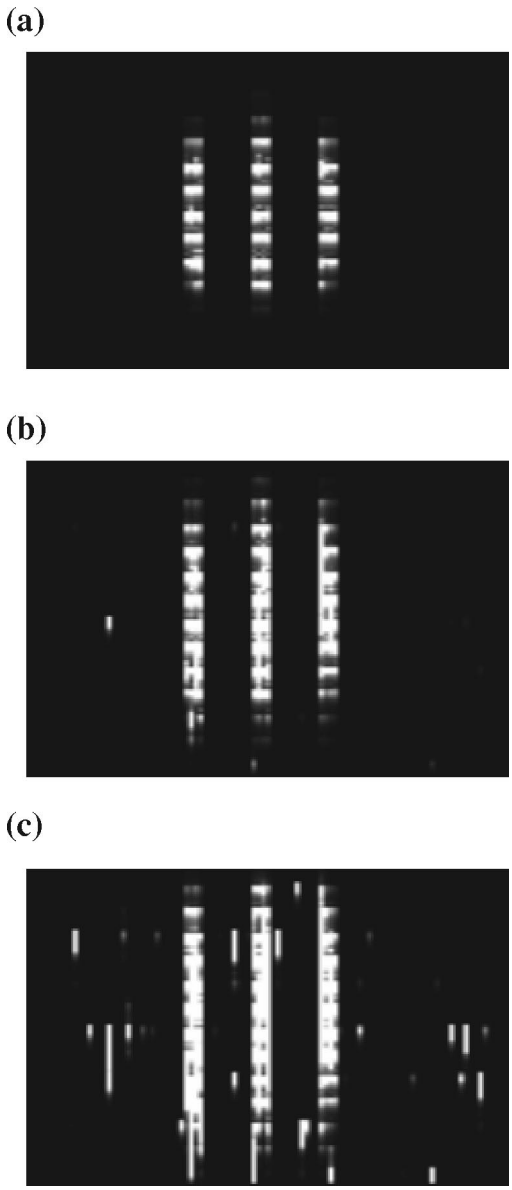

FIG. 6. Spatially dependent excitation of a motor ensemble by a broadband coherent light field.

comparison of the transition rate difference [Figs. 5(a,b)] and the current distributions [Figs. 5(c,d)] demonstrates that the transition rate difference is high where the currents are low and vice versa. The spatially localized transition rates consequently bridge the regions of negative currents given by the potential steps. As a result, a significant fraction of the molecular motors gets over the potential steps leading to an increased forward propagation of the motors.

As a second example we consider a ''broadband'' excitation, i.e., the parameter Γ is chosen such that all motors experience the same excitation—independent of their position with respect to the potential shape. The results are displayed in Fig. 6. The homogeneous excitation induces a transfer between the motor states—independent of their position relative to potential minima and maxima. As a consequence, the transition rates do not ''bridge the gaps'' defined by the current minima as efficiently as in the situation of Fig.

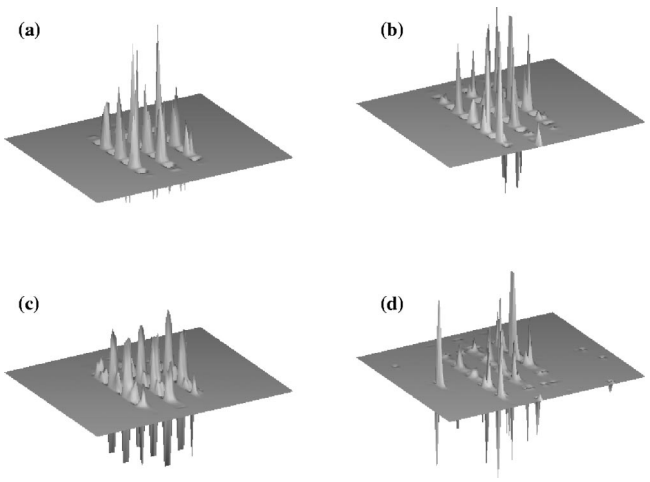

FIG. 7. Transition rates (a,b) and drift currents (c,d) for the ground-state motors immediately after the start of the calculation (a,c) and after 20 ms (b,d).

4. In combination with the dynamic interaction between bound and free motors this leads to a spatiotemporal broadening of the motor distribution. This effect can be further analyzed with temporal snapshots of the transition rate difference and drift currents. These distributions are (for the ground-state level) displayed in Fig. 7 immediately after the start of the calculation (a,c) and after 20 ms (b,d). Immediately after the start of the simulation [Figs. 7(a,c)] the spatial distribution of $\Delta\kappa_1$ [Fig. 7(a)] is—via its dependence on the motor density—rather uniform and reflects the regular accumulation of the motors as defined by the potential and the drift currents [Fig. 7(c)]. With increasing time, however, $\Delta\kappa_1$ [Fig. 7(b)] and the drift currents [Fig. 7(d)] change into irregular distributions with strong spatial fluctuations. It is this nonequilibrium excitation and relaxation dynamics that is responsible for the spatiotemporal motor distribution shown in Fig. 6.

IV. CONCLUSION

We have discussed the spatiotemporal dynamics of inhomogeneous molecular motor systems. A theoretical model has been set up that considers the interaction and coupling of bound and free motors, their selective optical excitation, and spatiotemporally varying molecular properties. It may represent a basis for a fundamental analysis of fluctuations, influence of external forces, collective behavior, and control on a mesoscopic level.

Early results on the simulation of spatially inhomogeneous optical molecular motors reveal the dependence of the system behavior on particle distribution, diffusive behavior, and spatiotemporal optical excitation. These results cannot give more than a first indication of possible simulations of real molecular systems. However, we are convinced that in particular the spatial and temporal resolutions of the model description as well as the explicit inclusion of spatial fluctuations in molecular properties (e.g., particle size and spatial positioning), noise and interaction strengths between the individual components on the spatiotemporal behavior of the system may principally allow the investigation and comparative analysis of real molecular motor systems.

For future investigations we plan to analyze the influence of spatial fluctuations in molecular properties (e.g., particle size and spatial positioning) and interaction strengths between the individual components on the spatiotemporal behavior of the system. This includes, e.g., the application of different noise and statistical functions for the individual parameters and the comparative analysis of their influence on the spatiotemporal behavior of the system.

APPENDIX

The numerical integration of the equations of motion (1) and (3) requires a simultaneous consideration of various time and length scales. This can be done on the basis of a finite difference method. Using the Hopscotch [70] method as a general scheme, the operators in the system of equations are discretized by the Lax-Wendroff [71] scheme. In the Lax-Wendroff scheme for finite-difference equations, the xy plane is divided into a grid with regular mesh size $\Delta x\Delta y$. Every variable is then represented by its values at the discrete set of points x_l, y_m, where $l=0,1,\ldots,N_x$ and $m=0,1,\ldots,N_y$. In the following, we will denote the discrete space dependence by subscripts (x is the propagation direction of the motors while the integration in discrete time intervals Δt is represented as superscripts, e.g., $(p^n_{l,m})$. After insertion of the expression for the current [Eq. (2)] into the Fokker-Planck equations for the motor molecules [Eqs. (1) and (3)], the equations of motion can be written in the following form:

$$\left(\frac{\partial}{\partial t}=a\frac{\partial^2}{\partial x^2}+b\frac{\partial^2}{\partial y^2}+c\frac{\partial}{\partial x}+d\right)p+e, \tag{A1}$$

where the coefficients (e.g., for the bound motors) are given by $a=b=\mu_i k_b T$, $c=\mu_i(\nabla V_i-F)$, $d=-\Gamma_{i\infty}-\Sigma_{j\neq i}\kappa_{ij}$, and $e=\Gamma_{\infty i}p_\infty+\Sigma_{j\neq i}\kappa_{ji}p_j$, respectively. Discretization of the operators leads to an *explicit finite-difference equation*:

$$\begin{aligned}\frac{1}{\Delta t}(p^{n+1}_{l,m}-p^n_{l,m})=a\frac{1}{2\Delta x}(p^n_{l+1,m}-2p^n_{l,m}+p^n_{l-1,m})\\ +b\frac{1}{2\Delta y}(p^n_{l+1,m}-2p^n_{l,m}+p^n_{l-1,m})\\ +c\frac{1}{2\Delta x}(p^n_{l+1,m}-p^n_{l-1,m})+dp^n_{l,m}+e.\end{aligned} \tag{A2}$$

In Eq. (A2), the (unknown) value of p with index m at the time step $n+1$ is explicitly related to the (known) values of p at the time step n. Next to the explicit form, we can relate the temporal change of the value of p with index m to the corresponding values at the time step $n+1$ leading to the *implicit finite-difference equation*:

$$\frac{1}{\Delta t}(p_{l,m}^{n+1}-p_{l,m}^{n})=a\frac{1}{2\Delta x}(p_{l+1,m}^{n+1}-2p_{l,m}^{n+1}+p_{l-1,m}^{n+1}) + b\frac{1}{2\Delta y}(p_{l+1,m}^{n+1}-2p_{l,m}^{n+1}+p_{l-1,m}^{n+1}) + c\frac{1}{2\Delta x}(p_{l+1,m}^{n+1}-p_{l-1,m}^{n+1})+dp_{l,m}^{n+1}+e. \tag{A3}$$

A suitable combination of explicit and implicit integrations allows one to reduce the discretization errors from both schemes: In the Hopscotch method the spatial grid points are divided into two classes: ''Even points'' with an even sum of the indices $l+m$ amd ''odd points'' where the sum $l+m$ is odd. After the initialization of the fields at the start of the calculation the values of the variables at even points are integrated according to the explicit integration scheme (A2) for one time step Δt. Then, the respective values at the odd points are calculated according to the implicit scheme (A3). In the next time-integration step the treatment of the odd and even points is reversed. In this second cycle, the odd points are first calculated on the basis of the explicit scheme. After that, the even points are solved following the implicit equations. These four alternating integration cycles are repeated until the end time of the simulation is reached. Following this procedure the discretization errors from the explicit and the implicit scheme resulting from the first-order approximation have opposite sign. They thus cancel as a consequence of the combination of both schemes. As an overall result the accuracy of the Hopscotch method becomes second order in time and space.

[1] T. Strick, J.-F. Allemand, V. Croquette, and D. Bensimon, Phys. Today **54**, 46 (2001).
[2] I. Rayment, H. Holden, M. Whittaker, C. Yohn, M. Lorenz, K. Holmes, and R. Milligan, Science **261**, 58 (1993).
[3] J. Abrahams, A. Leslie, R. Lutter, and J. Walker, Nature (London) **370**, 621 (1994).
[4] H. Noji, R. Yasuda, M. Yoshida, and J.K. Kinosita, Nature (London) **386**, 299 (1997).
[5] Y. Goldman, Cell **93**, 1 (1998).
[6] Y. Suzuki, T. Yasunaga, R. Ohkura, T. Wakabayashi, and K. Sutoh, Nature (London) **396**, 380 (1998).
[7] S. Block, Cell **93**, 5 (1998).
[8] C. Shingyoji, H. Higuchi, M. Yoshimura, E. Katayama, and T. Yanagida, Nature (London) **393**, 711 (1998).
[9] J. Gelles and R. Landick, Cell **93**, 13 (1998).
[10] R. Astumian, Science **276**, 2127 (1997).
[11] J. Prost, J.F. Chauwin, L. Peliti, and A. Ajdari, Phys. Rev. Lett. **72**, 2652 (1994).
[12] F. Jülicher, A. Ajdari, and J. Prost, Rev. Mod. Phys. **69**, 1269 (1997).
[13] C.S. Peskin, G.B. Ermentrout, and G. Oster, *Cell Mechanics and Cellular Engineering* (Springer, New York, 1994).
[14] R.D. Astumian and M. Bier, Phys. Rev. Lett. **72**, 1766 (1994).
[15] M.O. Magnasco, Phys. Rev. Lett. **72**, 2656 (1994).
[16] C.R. Doering, Nuovo Cimento **17**, 685 (1995).
[17] I. Derényi and T. Vicsek, Proc. Natl. Acad. Sci. U.S.A. **93**, 6775 (1996).
[18] H.X. Zhou and Y.D. Chen, Phys. Rev. Lett. **77**, 194 (1996).
[19] R.P. Feynman, R.B. Leighton, and M. Sands, *The Feynman Lectures on Physics* (Addison-Wesley, Reading, MA, 1999), Vol. 1.
[20] F. Jülicher and J. Prost, Phys. Rev. Lett. **75**, 2618 (1995).
[21] K. Sekimoto, J. Phys. Soc. Jpn. **66**, 1234 (1997).
[22] T. Shibata and S. Sasa, J. Phys. Soc. Jpn. **67**, 2666 (1998).
[23] I. Sokolov and A. Blumen, J. Phys. A **30**, 3021 (1997).
[24] F. Jülicher and R. Bruinsma, Biophys. J. **74**, 1169 (1998).
[25] T. Hondou, J. Phys. Soc. Jpn. **67**, 1818 (1998).
[26] H. Kamegawa, T. Hondou, and F. Takagi, Phys. Rev. Lett. **80**, 5251 (1998).
[27] M.O. Magnasco, Phys. Rev. Lett. **71**, 1477 (1993).
[28] A. Parmeggiani, F. Jülicher, A. Ajdari, and J. Prost, Phys. Rev. E **60**, 2127 (1999).
[29] M.E. Fisher and A. Kolomeisky, Proc. Natl. Acad. Sci. U.S.A. **96**, 6597 (1999).
[30] R. Lipowsky, Phys. Rev. Lett. **85**, 4401 (2000).
[31] F. Jülicher and J. Prost, Phys. Rev. Lett. **78**, 4510 (1997).
[32] G. Lattanzi and A. Maritan, Phys. Rev. E **64**, 061905 (2001).
[33] D. Keller and C. Bustamente, Biophys. J. **78**, 541 (2000).
[34] C.R. Doering, W. Horsthemke, and J. Riordan, Phys. Rev. Lett. **72**, 2984 (1994).
[35] S. Klumpp, A. Mielke, and C. Wald, Phys. Rev. E **63**, 031914 (2001).
[36] T. Elston and C. Peskin, SIAM (Soc. Ind. Appl. Math.) J. Appl. Math. **60**, 842 (2000).
[37] P. Reinmann, R. Kawai, C.V.D. Broeck, and P. Hänggi, Europhys. Lett. **45**, 545 (1999).
[38] Z. Csahok, F. Family, and T. Vicsek, Phys. Rev. E **55**, 5179 (1997).
[39] S. Leibler and D. Huse, J. Cell Biol. **121**, 1357 (1993).
[40] I. Derenyi and T. Vicsek, Phys. Rev. Lett. **75**, 374 (1995).
[41] I. Derenyi and A. Ajdari, Phys. Rev. E **54**, R5 (1996).
[42] R. Lipowsky, *Movements of Molecular Motors* (World Scientific, Singapore, 2001).
[43] V. Lisy and B. Brutovsky, Phys. Rev. E **61**, 4045 (2000).
[44] Y. Shao, A.V. Maximov, I. Ourdev, W. Rozmus, and C.E. Capjack, IEEE J. Quantum Electron. **37**, 617 (2001).
[45] A. Nilsson, P. Alsholm, A. Karlsson, and S. Andersson-Engels, Appl. Opt. **37**, 2735 (1998).
[46] A. Hoekstra and P. Sloot, Part. Part. Syst. Charact. **11**, 189 (1994).
[47] T. Pham, O. Coquoz, J. Fishkin, E. Anderson, and B. Tromberg, Rev. Sci. Instrum. **71**, 2500 (2000).
[48] W. Star, *Optical-Thermal Response of Laser-Irradiated Tissue* (Plenum, New York, 1995).
[49] J.B. Fishkin, S. Fantini, M.J. vandeVen, and E. Gratton, Phys. Rev. E **53**, 2307 (1996).
[50] I. Saidi, S. Jacques, and F. Kittel, Appl. Opt. **34**, 7410 (1995).
[51] K. Yee, IEEE Trans. Antennas Propag. **14**, 302 (1966).

[52] A. Dunn and R. Richards-Kortum, IEEE J. Sel. Top. Quantum Electron. **2**, 898 (1996).
[53] A. Dunn, C. Smithpeter, A. Welch, and R. Richards-Kortum, J. Biomed. Opt. **2**, 262 (1997).
[54] A. Taflove and M. Brodwin, IEEE Trans. Microwave Theory Tech. **23**, 623 (1975).
[55] L. Gorre, E. Ionannidis, and P. Silberzan, Europhys. Lett. **33**, 267 (1996).
[56] L. Gorre-Talini, J. Spatz, and P. Silberzan, Chaos **8**, 650 (1998).
[57] J. Rousselet, L. Salome, A. Ajdari, and J. Prost, Nature (London) **370**, 446 (1994).
[58] K. Mislow, Org. Chem. **2**, 151 (1989).
[59] B. Fergina, *Molecular Switches* (Wiley-VCH, Germany, 2001).
[60] J.-P. Sauvage and C. Dietrich-Buchecker, *Molecular Catenanes, Rotaxanes and Knots* (Wiley-VCH, Germany, 1999).
[61] V. Balzani, A. Credi, F. Raymo, and J. Stoddart, Angew. Chem., Int. Ed. **39**, 3348 (2000).
[62] T. Hugel, N. Holland, A. Cattani, L. Moroder, M. Seitz, and H. Gaub, Science **296**, 1103 (2002).
[63] B. Feringa, N. Koumura, R.V. Delden, and M.T. Wiel, Appl. Phys. A: Mater. Sci. Process. **A75**, 301 (2002).
[64] G. Gryndberg and C. Robillard, Phys. Rep. **355**, 335 (2001).
[65] A. Parmeggiani, F. Jülicher, L. Piliti, and J. Prost, Europhys. Lett. **56**, 603 (2001).
[66] Y. Okada and N. Hirokawa, Science **283**, 1152 (1999).
[67] A.D. Mehta, R.S. Rock, M. Rief, J.A. Spudich, M.S. Mooseker, and R.E. Cheney, Nature (London) **400**, 590 (1999).
[68] Z. Wang and M. Sheetz, Biophys. J. **78**, 1955 (2000).
[69] R.F. Fox and M.H. Choi, Phys. Rev. E **63**, 051901 (2001).
[70] I.S. Greig and J.D. Morris, J. Comput. Phys. **20**, 64 (1976).
[71] W.H. Press, B.P. Flannery, S.A. Teukolsky, and W.T. Vetterling, *Numerical Recipes—The Art of Scientific Computing* (FORTRAN Version) (Cambridge University Press, Cambridge, England, 1989), p. 64.